

## Extreme Red Sensitivity of ACS/WFC

Ronald L. Gilliland and Adam G. Riess

*Space Telescope Science Institute, 3700 San Martin Drive, Baltimore, MD 21218*

**Abstract.** Establishing the instrumental sensitivity as a function of wavelength within the domain covered by the F850LP ( $z$ ) filter is critical for a number of ACS science programs. Absolute sensitivity calibrations with hot white dwarfs showed that substantial updates up to 20% in the blue were needed relative to pre-flight estimates, and were suggestive of a significant gradient in the far-red (0.85–1.1 microns) QE update needed (but did not suffice to constrain this well). We report here observations of several hot white dwarfs; as well as a M7 V, a L3.5 V and a T6.5 V star in F625W, F814W and F850LP with ACS/WFC. The concentration of flux for the coolest stars to the longest wavelengths probed with F850LP provide a means of defining the quantum efficiency curve underlying this broad filter. We find, unique to the  $z$ -band filter, that over the range O, M, L, T stars that the encircled energy for small-to-moderate apertures can vary at the level of 10s of percent. Attempts to separate out underlying QE variations and wavelength dependent PSF effects are reported on here. For an L dwarf, similar in SED to a high redshift Type Ia SN, these effects can reach half a magnitude for small apertures.

### 1. Previous Sensitivity Update

Figure 1 shows the in-flight corrected throughput values for three filters with ACS/WFC (F625W, F814W and F850LP) as well as the overall throughput (labeled as CLEAR) for all non-filter components—with the underlying CCD Quantum Efficiency being the most limiting factor over this domain. The ratio of observed to predicted count rates for observations of spectrophotometric standards (GD71, GRW+70D5824) using pre-launch throughput values are shown in the lower panel for all the broadband filters. The generally smooth variation with wavelength suggested a wavelength dependent correction was needed for the CCD QE curve and the values shown in the upper panel incorporate such a change. QE values for wavelengths between the pivot wavelengths of the filters were set by spline interpolation; for lack of a better constraint updates to the QE curve used a linear extrapolation beyond 9100 Å (e.g., we assumed the pre-launch value drops by 10% by 10,400 Å). The spectrophotometric standards are hot white dwarfs, and thus have a flux distribution that tends to weight sensitivity determinations to the short wavelength end of filters.

**The remainder of this paper explores the validity of the existing throughput curve over the F850LP— $z$ -filter bandpass. Of particular interest is the throughput in the far red.**

### 2. Extreme Red Stars as Probe

Observations of very red stars with known spectrophotometry provide information on the wavelength distribution of sensitivity within the broad F850LP filter. We chose three stars with M, L and T spectral types for which flux-calibrated spectra are available from the literature. These are detailed in Table 1. For the L-dwarf a STIS spectrum is used.

Two factors are most important in determining sensitivity to faint stellar sources:

1. Encircled energy arising from possible PSF shape differences with wavelength.

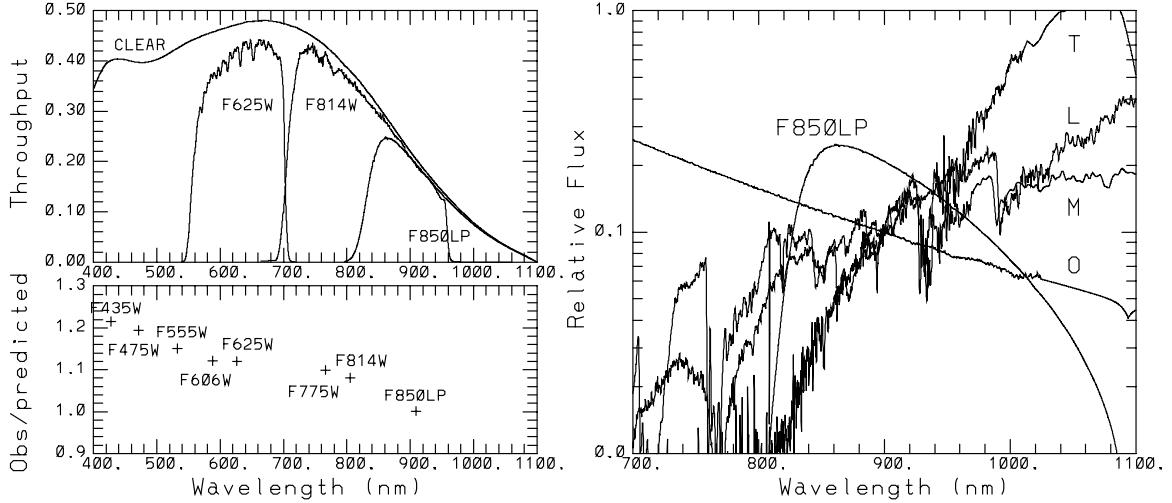


Figure 1. Left: Upper panel shows total system throughputs for CLEAR, F625W, F814W and F850LP filters following the updates to original CCD QE curves based on the initial observational results shown in the lower panel. Right: Relative fluxes for the O, M, L and T stars arbitrarily normalized to 0.1 at 9000 Å, and the F850LP sensitivity. The wavelength dependent contribution to counts changes dramatically for these stars as a function of wavelength.

Table 1. Red Star Data

Star	Type	RA	DEC	V	I <sub>c</sub>	z	Reference
VB 8	M7	16:55:34	-08:23.6	16.81	12.28	11.73	Reid 2002
2M0036+18	L3.5	00:36:16	+18:21.1	21.34	16.11	15.21	STIS(6797)
2M1237+65	T6.5	12:37:39	+65:26.2	>28.0	21.51	19.62	Burgasser et al. 2002

2. Establishing the correct underlying throughput as a function of wavelength.

### 3. Encircled Energy Changes

We have determined encircled energies within  $3 \times 3$ ,  $5 \times 5$  and  $9 \times 9$  pixel areas centered on the stars. Normalization is relative to an “infinite” aperture (really a radius of  $2''/8$ ) sum, and sky subtraction is based on the value within a surrounding annulus of 3.0–5.0 arcsec. For these tables we include entries for ‘ETC’—the encircled energy assumed by our current exposure time calculator, which is independent of input spectral type. The ‘Pivot lambda’ evaluates the photon flux weighted mean wavelength, i.e., the integral of  $QE \times F_{\lambda} \lambda^2$  divided by the integral of  $QE \times F_{\lambda} \lambda$ , each over  $\lambda$ .

Table 2. F625W Encircled Energy

Star	$3 \times 3$	$5 \times 5$	$9 \times 9$	Pivot $\lambda$
ETC	0.671	0.834	0.880	—
O	0.591	0.791	0.882	6249
M	0.590	0.792	0.886	6554
L	0.582	0.782	0.877	6654

For F625W there is no evidence of encircled energy changes as a function of spectral type. The drop in encircled energy at  $3 \times 3$  pixels for the stellar sources relative to ETC assumptions (based

on modeled PSFs) is explained by the use of drizzled (geometrically corrected) images for which the cores of PSFs experience minor smoothing. At the scale of  $9 \times 9$  pixels the smoothing inherent with drizzling is unimportant and the ETC and observed encircled energies agree well.

Table 3. F814W Encircled Energy

Star	$3 \times 3$	$5 \times 5$	$9 \times 9$	Pivot $\lambda$
ETC	0.609	0.797	0.880	—
O	0.548	0.756	0.874	7949
M	0.520	0.727	0.860	8429
L	0.492	0.708	0.850	8597
T	0.483	0.699	0.861	8954

For F814W a progressive broadening of the PSF at the smallest aperture size is evident and amounts to a loss of 12% in effective sensitivity from a very blue to a very red star. At the larger  $9 \times 9$  aperture size the differences are consistent with measurement error.

Table 4. F850LP Encircled Energy

Star	$3 \times 3$	$5 \times 5$	$9 \times 9$	Pivot $\lambda$
ETC	0.588	0.757	0.880	—
O	0.481	0.679	0.829	9020
M	0.430	0.632	0.800	9303
L	0.425	0.614	0.783	9425
T	0.355	0.526	0.692	9846

For the F850LP filter PSF changes on all scales are significant. In particular for the  $3 \times 3$  aperture relevant for detection of sources near the faint limit, an L-dwarf (similar in spectral energy distribution to a Type Ia SN with  $z \sim 2$ ) would have a throughput down by  $0.425/0.588 = 0.72$  compared to the ETC PSF. Even at the larger  $9 \times 9$  pixel aperture the loss is  $0.783/0.88 = 0.89$  relative to expectations of the Exposure Time Calculator.

**At the extreme-red wavelengths covered by the F850LP filter a significant “red halo” effect has set in. Even at a radius of 1.0 arcsec the encircled energy for the T dwarf is down by 5% relative to a blue star, perhaps more if the red halo places flux beyond our 2.8 arcsec normalization aperture.**

#### 4. Quantum Efficiency With $\lambda$

The second major component in setting the far-red sensitivity for the ACS/WFC is to quantify the underlying CCD QE over the 8500 Å to 11000 Å domain. Recall (see Figure 1) that a linear extrapolation based on observed values weighted toward shorter wavelengths had been applied in this domain. With observations of extremely red stars we can now test more directly for the wavelength dependence of QE.

We now take sums over large apertures,  $2''8$  radius in the observations, and use the  $101 \times 101$  pixel sums from the ETC of similar size to provide expected count rates using known spectra. As before sky is defined over a 3.0–5.0 arcsec annulus and subtracted.

The following table shows observed to expected count rate ratios in an “infinite” aperture using the current wavelength dependent sensitivities.

The ground-based M-dwarf flux is evidently  $\sim 20\%$  too low (a similar offset was found for a ground-based L-dwarf spectrum—Reid et al. 2000—compared to STIS). We hypothesize the need

Table 5. Ratio of Observed to Expected Counts—Infinite Aperture

Star	F625W	F775W	F814W	F850LP	F850LP/F814W
O	0.984	0.982	0.976	0.942	0.965
M	1.178	1.108	1.201	1.125	0.937
L	0.972	0.926	0.964	0.859	0.891
T	—	1.5::	1.162	0.971	0.836

for linearly dropping the CCD QE over the 9500–11000 Å domain and solving for the slope that yields near unity for all stars in the ratio F850LP/F814W (we effectively use the F814W observations to normalize the zero point in the spectrophotometry). We find that fixing the current value up to 9500 Å and applying a slope of  $-3.8 \times 10^{-4}$  per Å (i.e., sensitivity at 10000 Å is set at 81% of current value) results in F850LP/F814W ratios of 0.995, 1.007, 0.974, 1.024 for the O, M, L, T stars respectively. The “solution” while effective is not unique, as equally good (close to unity ratios throughout) results follow from a range of starting  $\lambda$  and slopes for the linear drop of far-red QE.

## 5. Summary

The far-red sensitivity needs to be adjusted for both a wavelength dependent encircled energy (for which these observations determine well) and for a possible wavelength dependent term in the Quantum Efficiency (which these observations provide a good provisional solution).

For a mid-L dwarf which serves as a good analogue for  $z \sim 2$  Type Ia Supernova we find implied sensitivity losses of 28% due to encircled energy in a  $3 \times 3$  pixel aperture and 10% from an additional QE adjustment over the  $z$ -band. Combined, this equates to a 0.47 magnitude loss in sensitivity for such an extremely red target compared to current ETC/Synphot predictions. These results show that for the F850LP filter, count rate estimates need to take into account a PSF that is a strong function of the underlying spectral energy distribution for the observed target. The CCD QE will be updated to reflect the inferred drop beyond 9500 Å. The dependence of encircled energy with underlying spectrum for F850LP will require compensation by the observer for ETC estimates and photometry.

**Acknowledgments.** We thank Ralph Bohlin, Guido DeMarchi, Neill Reid, Marco Sirianni and Zlatan Tsvetanov for input at various stages.

## References

- Burgasser, A. J., et al. 2002, AJ, 123, 2744  
 Reid, I. N., et al. 2000, AJ, 119, 369  
 Reid, I. N. 2002, private communication